Time Domain Reflectometry Surface Reflections for Dielectric Constant in Highly Conductive Soils

Renpeng Chen[1]; Vincent P. Drnevich, F.ASCE[2]; Xiong Yu, M.ASCE[3]; Robert L. Nowack[4]; and Yunmin Chen[5]

Abstract: This paper presents a model-based approach to determine dielectric constants from time domain reflectometry (TDR) measurement in highly conductive soils. It makes use of information contained in the TDR signal from the reflection at the surface of the soil rather than the reflection from the end of the probe. The TDR method is widely used to determine the volumetric water content of soils. Commonly used information from the TDR signals includes the apparent dielectric constant and the electrical conductivity. The apparent dielectric constant is generally measured by analyzing the travel time of electromagnetic waves reflected from the end of the soil probe. In soils with high electrical conductivities, the attenuation of the signal can eliminate the reflection from the end of the probe, which limits the application of TDR to these materials. A simplified frequency-independent dielectric model is utilized to invert the dielectric constant from the reflected signals at the soil surface. Results indicate that the dielectric constant can be determined with reasonable accuracy by the proposed approach for soils with high electrical conductivity, where the conventional travel time analysis fails due to significant signal attenuation.

DOI: 10.1061/(ASCE)1090-0241(2007)133:12(1597)

CE Database subject headings: Dielectric constant; Electrical conductivity; Electrical resistivity; Soil properties; Travel time.

Introduction

Time domain reflectometry (TDR) technology is a reliable, fast, and safe technology for measuring soil volumetric water content (Benson and Bosscher 1999; Noborio 2001). Fig. 1 shows the main sections of TDR, including the step generator, data acquisition system, coaxial cable, and measurement probe. The step generator sends a step voltage to the coaxial cable, the input signal and the reflected signal are recorded by the data acquisition system, and the apparent dielectric constant and the DC electrical conductivity are estimated from the recorded signal.

A "universal" calibration equation relating the volumetric water content of soils to the TDR-measured soil apparent dielectric constant (Topp et al. 1980) is widely used in engineering practice. Siddiqui and Drnevich (1995) and Yu and Drnevich (2004a) presented efforts to extend the application of TDR to measure the gravimetric water content and the dry density of soils for geotechnical engineering applications. A special multiple-rod probe was designed for measurement in compacted fills and embankments in conjunction with a cylindrical mold probe. This design is more suitable for repeated installation and withdrawal (Siddiqui and Drnevich 1995). An ASTM standard method, designated as D 6780, describes the details of this method (ASTM 2005b).

Recently, Yu and Drnevich (2004b) and Chen et al. (2006) applied TDR to the compaction control of chemically modified soils. It was observed that estimation of the dielectric constant using travel time analysis is challenging because the chemically modified soils can be highly conductive, which causes significant energy attenuation (Topp et al. 1980, 2000; Jones and Or 2004). This makes it almost impossible to use conventional travel time analysis, which involves determining the reflection from the end of the probe for these soils and other highly conductive soils such as fat clays. Insulating the TDR probes with a dielectric coating is an effective way to reduce energy attenuation, but this also brings the undesirable effects of reduced sensitivity and the loss of information for the electrical conductivity.

Jones and Or (2004) used resonant frequency analysis and fitting of the scatter function for highly conductive soils, which extended the application range of the TDR method. The optimal probe length, however, was determined to be as short as 30 mm for frequency domain analysis; short probes were found to suffer from reduced accuracy (Jones and Or 2004).

Extraction of information from the TDR signals relies on an increased understanding of the wave propagation phenomena in the TDR system. Heimovaara et al. (1994) and Jones and Or (2004) developed theoretical models for a matched TDR probe.

[1]Professor, Key Laboratory of Soft Soil and Geoenvironment, Ministry of Education, 38 Zheda Rd., Hangzhou, 310027, China. E-mail: chenrp@zju.edu.cn

[2]Professor, School of Civil Engineering, Purdue Univ., 550 Stadium Mall, West Lafayette, IN 47907-2051 (corresponding author). E-mail: drnevich@purdue.edu

[3]Assistant Professor, Dept. of Civil Engineering, Case Western Reserve Univ., Cleveland, OH 44106-7201. E-mail: xiong.yu@case.edu

[4]Professor, Dept. of Earth and Atmospheric Sciences, Purdue Univ., 550 Stadium Mall Dr., West Lafayette, IN 47907. E-mail: nowack@purdue.edu

[5]Professor, Key Laboratory of Soft Soil and Geoenvironment, Ministry of Education, 38 Zheda Rd., Hangzhou, 310027, China. E-mail: chenyunmin@zju.edu.cn

Note. Discussion open until May 1, 2008. Separate discussions must be submitted for individual papers. To extend the closing date by one month, a written request must be filed with the ASCE Managing Editor. The manuscript for this paper was submitted for review and possible publication on December 14, 2005; approved on October 31, 2006. This paper is part of the ***Journal of Geotechnical and Geoenvironmental Engineering***, Vol. 133, No. 12, December 1, 2007. ©ASCE, ISSN 1090-0241/2007/12-1597–1608/$25.00.

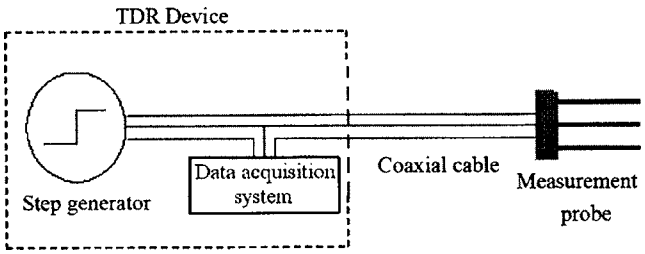

Fig. 1. Example of TDR system (adapted from Drnevich et al. 2001)

Yanuka et al. (1988) presented a model that accommodated multiple reflections in an unmatched TDR system. The dielectric permittivity was assumed to be a constant. Feng et al. (1999) combined the work of Yanuka et al. (1988) and Heimovaara et al. (1994) to formulate electromagnetic wave propagation in a nonuniform TDR system as a feedback linear-time-invariant system. Lin (2003) developed a general model for a nonuniform system using the concept of an input impedance transform.

This paper presents a model-based approach to determine dielectric constants from TDR measurement in highly conductive soils. The approach utilizes information contained in the TDR signal from the reflection at the surface of the soil and employs the numerical model for the propagation of the TDR signals in a nonuniform transmission line embedded in a dispersive material by Lin (2003). The system parameters are first determined from a calibration process. After the system is calibrated, a two-parameter dielectric model is used to estimate the dielectric constant of soils by matching the predicted surface reflection versus the measured signal. Satisfactory results are obtained using this approach. Work in this paper can potentially extend the applications of TDR to the determination of water content and density in highly conductive soils such as chemically modified soils.

Theoretical Background

Model of TDR System Based on Transmission Line Theory

The propagation of a TDR signal in the TDR system is described by transmission line theory. To account for the behavior of an unmatched system, the TDR system can be discretized as a lumped circuit consisting of uniform sections (Fig. 2). Each section accounts for the front panel, cable, probe head, and probe, respectively. Under the assumption of a transverse electromagnetic propagating wave mode, the general solution for the transmission line equation in terms of voltage, V, and current, I, in complex phasor form is (Ramo et al. 1994)

$$V(z) = V^+ e^{-\gamma z} + V^- e^{\gamma z} \tag{1a}$$

$$I(z) = \frac{V^+}{Z_c} e^{-\gamma z} - \frac{V^-}{Z_c} e^{\gamma z} \tag{1b}$$

where z=position along the line; V^+ and V^-=two unknown voltage constants, which can be obtained using boundary conditions; γ=propagation constant, which is a complex quantity; and Z_c=characteristic impedance, depending only on the geometry of the line and the material characteristics of the dielectrics between the two conductors. The variables of γ and Z_c can be expressed as

$$\gamma = \frac{j\omega}{c}\sqrt{K^*} \tag{2a}$$

$$Z_c = \frac{Z_p}{\sqrt{K^*}} \tag{2b}$$

in which $j^2=-1$; ω=angular frequency; K^*=relative dielectric permittivity (dielectric permittivity ε^* normalized by the dielectric permittivity of free space ε_0 [$\varepsilon_0=8.85418\times10^{-12}$ F/m]); c=velocity of light in vacuum ($c=2.998\times10^8$ m/s); and Z_p=reference characteristic impedance, which is defined as the characteristic impedance of the transmission line insulated with air. The reference characteristic impedance can be calculated from the geometry of the line.

The cascade of a uniform transmission line depicted in Fig. 2 includes n sections, each with two unknown quantities (V^+ and V^-). There are altogether $2n$ unknowns to determine. The continuity conditions at the $(n-1)$ junctions between the different sections yield $2(n-1)$ equations [Eq. (3)]

$$V_i^+ e^{-\gamma_i l_i} + V_i^- e^{\gamma_i l_i} = V_{i+1}^+ + V_{i+1}^-; \quad i = 1 \cdots n-1 \tag{3a}$$

$$\frac{V_i^+}{Z_{c,i}} e^{-\gamma_i l_i} - \frac{V_i^-}{Z_{c,i}} e^{\gamma_i l_i} = \frac{V_{i+1}^+}{Z_{c,i+1}} - \frac{V_{i+1}^-}{Z_{c,i+1}}; \quad i = 1 \cdots n-1 \tag{3b}$$

The boundary conditions at the source and the end of the transmission line give another two equations

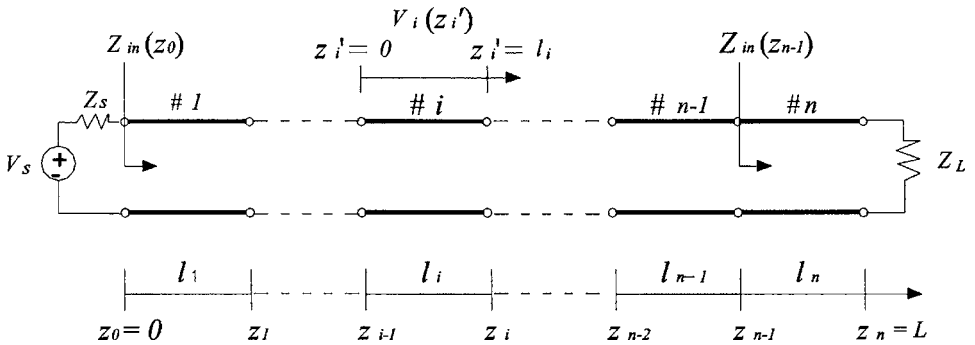

Fig. 2. Cascade of uniform sections used to represent a multisection transmission line. Each uniform section (i) is characterized by its propagation constant (γ_i), characteristic impedance ($Z_{c,i}$), and length (l_i) (adapted from Lin 2003).

$$V_1^+ + V_1^- = V_s - Z_s I(0) \tag{4a}$$

$$V_n^+ e^{-\gamma_n l_n} + V_n^- e^{\gamma_n l_n} = Z_L I(L) \tag{4b}$$

where V_s=source voltage; Z_s=source impedance, which is typically 50 ohms for the TDR device; and Z_L=load impedance at the end of the probe.

The $2n$ unknowns (V_i^+, V_i^-) in the transmission line equations can be solved using the $2n$ equations in Eqs. (3) and (4). The algorithm starts from the bottom (end) and works up, as shown in Eq. (5)

$$Z_{in}(z_n) = Z_L$$

$$Z_{in}(z_i) = Z_{c,i+1}\frac{Z_{in}(z_{i+1}) + Z_{c,i+1}\tanh(\gamma_{i+1}l_{i+1})}{Z_{c,i+1} + Z_{in}(z_{i+1})\tanh(\gamma_{i+1}l_{i+1})}$$

$$\vdots$$

$$Z_{in}(0) = Z_{c,1}\frac{Z_{in}(z_1) + Z_{c,1}\tanh(\gamma_1 l_1)}{Z_{c,1} + Z_{in}(z_1)\tanh(\gamma_1 l_1)} \tag{5}$$

where $Z_{c,i}$, γ_i, and l_i=characteristic impedance, propagation constant, and length of the ith section; and $Z_{in}(z_i)$=input impedance, which is the equivalent impedance when looking into the circuit at position z_i.

To facilitate the solution of the equations, Lin (2003) introduced a procedure based on the calculation of the transformed input impedance [Eq. (6)]. Using the transformed input impedance, the sampling voltage for the TDR system,$V(0)$, can be expressed as

$$V(0) = \frac{Z_{in}(0)}{Z_s + Z_{in}(0)}V_s \tag{6}$$

This is the sampled voltage in the frequency domain. The inverse fast Fourier transform can then be employed to obtain the time domain signals.

A concept commonly used in nonuniform transmission line is the reflection coefficient. The complex reflection coefficient at the interface between two sections, ρ_i, is expressed as (Ramo et al. 1994)

$$\rho_i = \frac{Z_{c,i+1} - Z_{c,i}}{Z_{c,i+1} + Z_{c,i}} = \frac{\frac{Z_{p,i+1}}{\sqrt{K_{i+1}^*}} - \frac{Z_{p,i}}{\sqrt{K_i^*}}}{\frac{Z_{p,i+1}}{\sqrt{K_{i+1}^*}} + \frac{Z_{p,i}}{\sqrt{K_i^*}}} \tag{7}$$

Relative Dielectric Permittivity of Materials

In order to predict a signal using Eq. (6), information on the relative dielectric permittivity of the soil surrounding the transmission line is needed. The relative dielectric permittivity is a frequency-dependent complex number, typically represented as

$$K^*(\omega) = K'(\omega) - jK''(\omega) \tag{8}$$

where the real part, K'=measure of the polarizability of the material; and the imaginary part, K'', represents the energy absorption or dielectric loss.

Several factors contribute to the energy loss. One part of the energy loss results from the fact that constituent dipolar molecules require a finite time, or relaxation time, to adjust to the changing electromagnetic fields (Debye 1929). A phase lag between the imposed field and the material's response then occurs. This phase lag is a function of the frequency of the applied field and causes a conversion of electromagnetic energy into heat.

In addition to the dielectric loss of the material, the electromagnetic energy can also be dissipated by electrical conduction, which is sometimes referred to as Ohmic losses. This conduction can be in the form of surface conduction via the electric charges on the surfaces of the solids and liquid phase ionic conduction via the dissolved electrolytes in the water phase (Santamarina et al. 2001). The expression of material dielectric permittivity accounting for these two energy attenuation mechanisms is (Krauss 1984)

$$K^*(\omega) = K'(\omega) - j\left(K''(\omega) + \frac{\sigma_{DC}}{\omega\varepsilon_0}\right) \tag{9}$$

where $K'(\omega)$ and $K''(\omega)$=real and imaginary parts of the relative dielectric permittivity; σ_{DC}=DC electrical conductivity; and ω=angular frequency.

One observation from Eq. (9) is that the effect of DC electrical conductivity, σ_{DC}, on the complex permittivity is strongly dependent on the frequency. The DC conductivity has a strong influence on the imaginary part of the permittivity at low frequencies; whereas at high frequencies the influence is less pronounced. Topp et al. (2000) discussed the relative contribution to the imaginary part of the dielectric permittivity by the dielectric relaxation and the electrical conductivity. Also, the long-term TDR waveform amplitudes are related to the electrical conductivity of the materials (Giese and Tiemann 1975; Topp et al. 1988).

While TDR is a broadband measurement tool that covers a frequency range from megahertz to gigahertz, the effective measurement frequency of commonly used TDR systems has been found to be in the low gigahertz range (Heimovaara 1994; Lin 2003). This range is beyond the upper bound of relaxation frequencies of bound water and Maxwell-Wagner effects (Hilhorst and Dirkson 1994; Santamarina et al. 2001). Heimovaara et al. (1994) found that the apparent dielectric constant measured with travel time analysis is mainly affected by the high-frequency components within the TDR frequency range. The relatively high effective measurement frequency makes results of TDR relatively stable for many types of soils.

Apparent Dielectric Constant K_a and Surface Reflection Apparent Dielectric Constant K_{aSR}

The apparent dielectric constant K_a measured by TDR is based on travel time analyses, where the reflections are determined from an empirical tangent line or other constructions applied to the signal returning from the end of the probe. It is different from the concept of dielectric constant commonly used in electrical engineering. This is also the reason that it is generally referred as "apparent" by TDR researchers.

The complex relative dielectric permittivity of a given material can be represented by Eq. (9). The total round trip travel time, Δt, for a transverse electromagnetic (TEM) wave propagating in an open-ended transmission line of length L_p imbedded in a medium with unit permeability and relative permittivity K^* is given by von Hippel (1954)

$$\Delta t = \frac{2L_p}{c}\sqrt{\left[K'(\omega)\left(1 + \sqrt{1 + \left(\frac{K''(\omega) + \frac{\sigma_{DC}}{\omega\varepsilon_0}}{K'(\omega)}\right)^2}\right)\right]\Bigg/2} \tag{10}$$

TDR travel time measurements give the apparent dielectric constant, K_a, as defined as

$$K_a = \left(\frac{c\Delta t}{2L_p}\right)^2 \tag{11}$$

Comparing Eqs. (10) and (11) indicates that both the real and imaginary components contribute to the value of K_a

$$K_a(\omega) = \frac{K'(\omega)\left(1+\sqrt{1+\left(\frac{K''(\omega)+\frac{\sigma_{DC}}{\omega\varepsilon_0}}{K'(\omega)}\right)^2}\right)}{2} \tag{12}$$

The apparent dielectric constant thus incorporates the contributions from both the dielectric relaxation and the electrical conductivity. This explains why increasing electrical conductivity causes the overestimation of the apparent dielectric constant.

The definition of surface reflection dielectric constant, K_{aSR}, proposed in this paper uses the real portion of Eq. (8)

$$K_{aSR} = K'(\omega \approx \textit{highest frequencies in the surface reflections}) \tag{13}$$

The matching process utilizes reflections from the soil surface which are mostly influenced by highest frequency components (Heimovaara et al. 1994). The dielectric relaxation $K''(\omega)$ in Eq. (8) is relatively small and is assumed to be zero (data to be provided later in the paper demonstrate the effects of this assumption). With these assumptions, Eq. (9) reduces to

$$K^*(\omega) = K_{aSR} - j\left(\frac{\sigma_{DC}}{\omega\varepsilon_0}\right) \tag{14}$$

which is the model used for inversion of the surface reflection. The advantage of using this approach is that it removes the influence of the DC electrical conductivity on K_{aSR} (data to be provided later in the paper also show that pore-water conductivities have virtually no influence on the signal reflected from the soil surface). Additional advantages of this model include its simplicity and the ability to be incorporated in inversion analysis to determine the most important information from the TDR signal, the real part of the dielectric permittivity at high frequencies.

TDR System and Observed Signal Reflections from Soil Surface

The TDR system used in this study includes a pulse generator with an integrated data acquisition system, a coaxial cable, a coaxial head, and a cylindrical mold probe. The coaxial head is a transition device from the coaxial cable to the measurement probe (Fig. 3). As described in ASTM standard D 6780-05 (ASTM 2005b), the soil was first compacted into the cylindrical mold fitted with a nonmetallic bottom plate and a rod was then driven into the mold along the central axis. The rod acted as the inner conductor of a "coaxial cable," while the cylindrical metal mold acts as the outer conductor. A ring collar was placed on top of the mold and the coaxial head was then placed on the ring. The diameter of the central rod and the inside diameter of the cylinder are 8 and 102 mm, respectively; the height of the cylindrical mold is 116 mm.

In-house-developed computer software was used to automate the TDR signal acquisition and interpretation (Yu and Drnevich 2004a; Daita et al. 2005). Fig. 4 shows a typical TDR signal. The

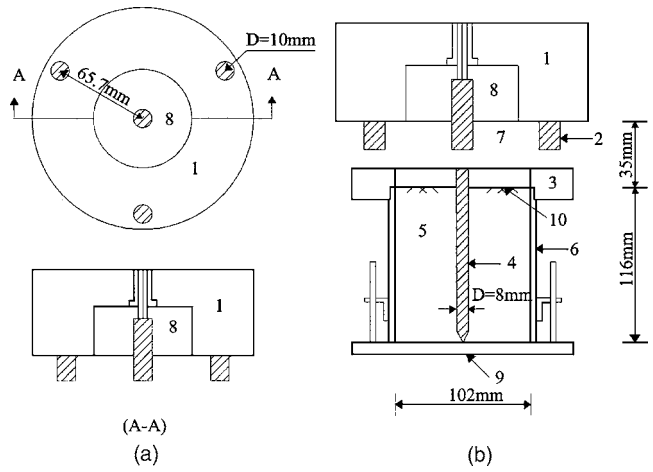

Fig. 3. Configuration of (a) coaxial head; (b) coaxial cylinder 1: stainless steel in the coaxial head; 2: studs; 3: stainless steel ring; 4: central rod; 5: soil or water in the mold; 6: metal mold; 7: air gap; 8: Delrin as the insulating material in the coaxial head; 9: Delrin as the base of the mold; 10: soil or water surface.

methods for estimating the apparent dielectric constant (K_a) by travel time analysis and the DC electrical conductivity (σ_{DC}) used by Giese and Tiemann (1975) are illustrated in Fig. 4, where L_p=probe length inserted into the mold; Δt=round-trip travel time along the probe; V_s=source voltage, which equals twice the step pulse; V_f=long-term voltage level; and C=constant related to probe configuration, which can be obtained by calibration or theoretical analysis. In Fig. 4, the first drop of the waveform from the interface of the air dielectric is mainly influenced by the high-frequency dielectric permittivity of the soil (Fellner-Feldegg 1969; van Gemert and De Graan 1972; Giese and Tiemann 1975; Clarkson et al. 1977).

Two data acquisition modes are set for the measurements of the dielectric constant and the conductivity. The time resolution of the TDR is set to 2.60×10^{-11} s for the measurement of the dielectric constant and 6.5×10^{-11} s for the measurement of the conductivity, corresponding to Nyquist frequencies of 19.2 and 7.7 GHz, respectively. The Nyquist frequencies of the two digitized signals are well above the upper limit of the frequency bandwidth of TDR to ensure complete information is obtained. The TDR waveforms for measurements in a mold partly filled with deionized water to different heights are plotted in Fig. 5. Also

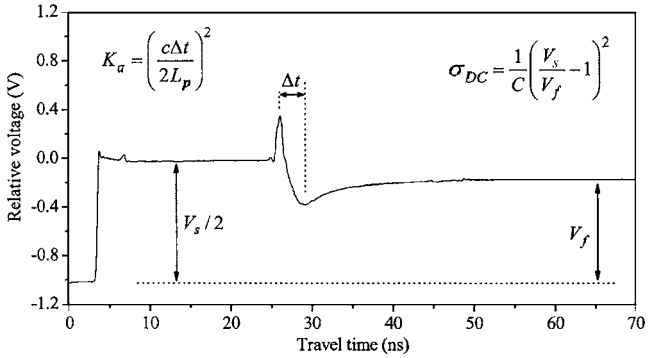

Fig. 4. A typical TDR waveform and methods for estimating apparent dielectric constant from travel time analysis and DC electrical conductivity from long-term DC level

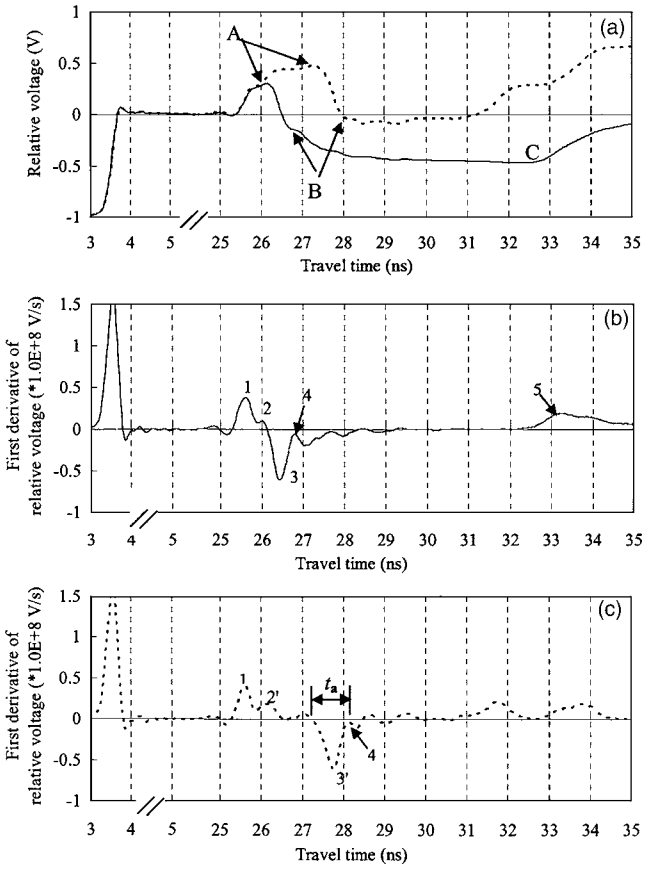

Fig. 5. TDR waveforms measured in deionized water: (a) TDR waveforms; (b) the first derivative of the TDR waveforms measured in a 116 mm long mold with a 35 mm long air gap (short air gap); and (c) the first derivative of TDR waveforms measured in a 250 mm long mold with a 235 mm long air gap (long air gap). In (a), the solid line is the TDR waveform for the short air gap, while the dash-dotted line is the TDR waveform for the long air gap. A: peak of relative voltages; B: point which is regarded as the end of first reflection on the waveform of the step response; C: first reflection from probe end on the waveform of the step response. In (b) and (c), 1: reflection from the coaxial head and the cable interface; 2 and 2′: reflection from the coaxial head and the air gap interface; 3 and 3′: first reflection from the water surface; 4: point which is regarded as the end of first reflection on the waveform of impulse response, corresponding to Point B on the waveform of the step response; 5: reflection from the probe end; A: Peak of the relative voltage; B: point which is regarded as the end of first reflection on the waveform of the step response; C: first reflection from probe end on the waveform of the step response.

plotted are the first derivatives of the original signals. The first derivative was calculated using the method of Svitzky and Golay (1964). The recorded waveform is the step response of the TDR system because the input signal is a step function. The first derivative of the waveform can be regarded as the impulse response of the TDR system, because the first derivative of the input step signal is an impulse.

In Fig. 5(a), the solid line is the TDR waveform for the deionized water when the 116 mm long probe is completely filled with deionized water. A 35 mm long air gap exists between the probe head and the water surface (Fig. 3). The dashed line is the TDR waveform using a 250 mm long probe, which is partially filled with deionized water. A 235 mm long air gap exists between the probe head and the water surface. The long air gap is used to identify and separate the reflections from the coaxial head and the surface of the water. Peaks 1 and 2′ in Fig. 5(c) indicate that the coaxial head and air gap have positive reflection amplitudes. The reflected signal from the water surface [peak 3 in Fig. 5(b) and peak 3′ in Fig. 5(c)] are negative because of the small characteristic impedance of water compared with those for the sections with the air gap and the probe head. When the length of the air gap is short, the reflections from the coaxial head, air gap, and surface of the water interfere with each other, as shown by peaks 1, 2, and 3 in Fig. 5(b).

The TDR waveforms of different materials are strongly influenced by their dielectric constants as presented in Fig. 6. For the oven-dried grundite (an illitic clay) [Curve W1 in Fig. 6(a)], the dielectric constant is small (K_a=2.3), which results in a low amplitude of the soil surface reflection. Meanwhile, the dielectric constant of water is high (K_a=79) [Curve W6 in Fig. 6(a)], which results in a large amplitude of the water surface reflection. The travel time of the wave in the different sections of coaxial head has about the same order as the rise time. This causes the reflection from water or the soil surface to overlap with the reflection from the air gap. Therefore, the position of point A in Fig. 5(a) on the step response is strongly influenced by the reflection from the soil (or water) surface, especially, the dielectric constant of the soil (or water).

The time difference between points A and C in Fig. 5(a) is the round-trip travel time of the wave along the probe in the soil or water specimen. Many methods have been developed to find point C (Timlin and Pachepsky 1996). Point A, the peak point on the waveform, is usually regarded as the first arrival of the reflection from the soil (or water) surface. However, because the amplitude of the reflection from the surface of soils with a low dielectric constant is small, this can introduce error in the determination in the first reflection because the peak will be controlled by the reflection of the coaxial head and air gap [see the shift of points A in Fig. 5(a)]. The shorter travel time can then lead to an underestimate of the dielectric constant.

Alternative methods of finding the first reflection include (1) use materials with a high dielectric constant (for instance, deionized water) to calibrate the system and find the first reflection point A; (2) find the soil surface reflection on the impulse response [peak point 3 in Fig. 5(b)] and subtract the half-width of the surface reflection impulse, $t_a/2$ from the time coordinate of point 3 from the cable-probe head reflection on the impulse response (peak Point 1) and add the travel time between the probe head and the soil surface to the time coordinate of the Point 1 [Fig. 5(b)]; and (4) develop improved probe head designs to minimize interference.

TDR System Calibration and TDR Waveform Simulation

TDR System Calibration

Theoretically, the characteristic impedance of the transmission line can be calculated from the geometry and the dielectric parameters of the insulating material. However, the multisection transmission line is an idealized model, which cannot account for the various factors in a real TDR system. Besides, the geometry of the sections and the properties of the dielectric material may also vary within the same section. These can be potential sources of error in simulating the TDR system response. Feng et al.

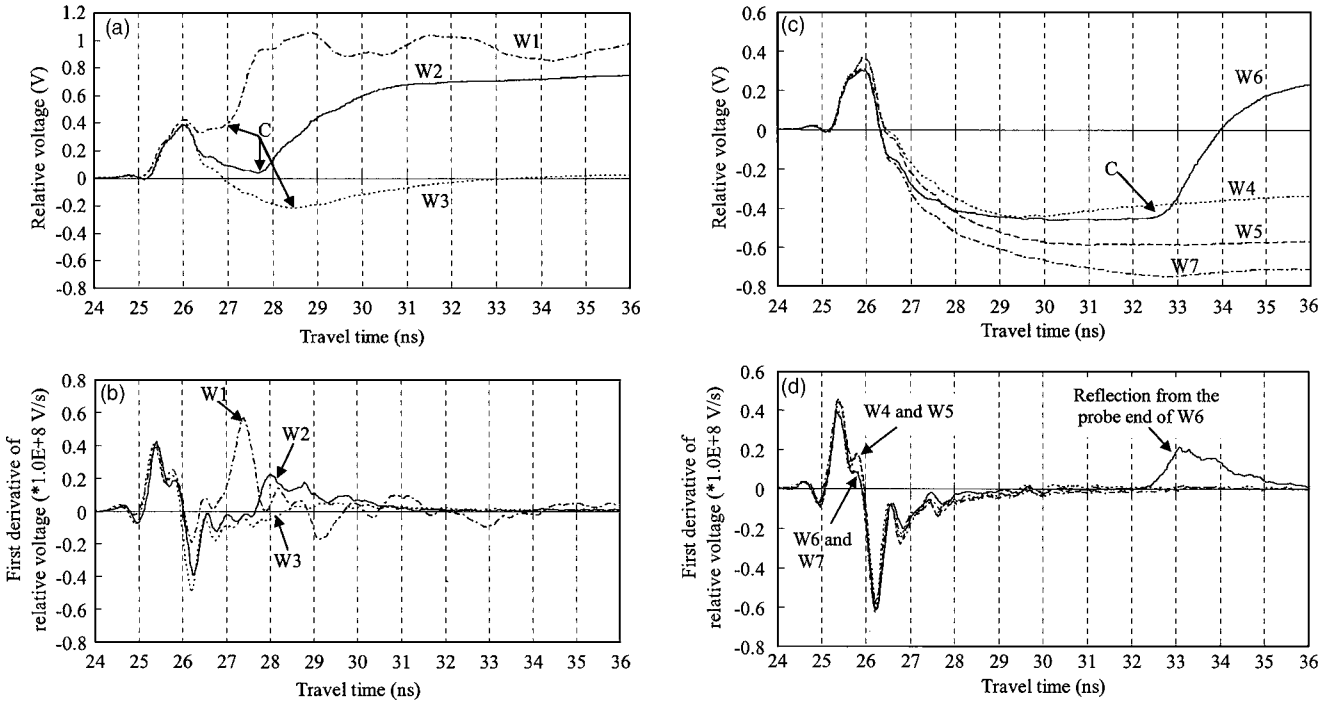

Fig. 6. Family of TDR measured waveforms for grundite and water: (a) signals for tests with low water contents; (b) derivatives of signals in (a); (c) signals for tests with high water contents and for deionized water; (d) derivatives of signals in (c). W1: waveform for the oven-dried grundite with a water content of 0%, K_a=2.3; W2: waveform for the grundite with a water content of 7%, K_a=5.4; W3: waveform for the grundite with a water content of 10%, K_a=15.3; C: first reflection from probe end on the waveform of step response; W4: waveform for 15% lime kiln dust modified grundite with a water content of 20.75% measured 63 hours after compaction, K_a=21; W5: waveform for 15% lime kiln dust modified grundite with a water content of 20.88% measured just after compaction. (The measurement of the dielectric constant with travel time analysis failed.) W6: waveform for deionized water, K_a=79; W7: waveform in salty water with an electrical conductivity of 476 mS/m. (The measurement of the dielectric constant with travel time analysis failed.)

(1999) and Lin (2003) used a calibration method to estimate the system parameters based on an optimization approach. This procedure is used in this study to calibrate the TDR system. The purpose of optimization is to obtain the best parameters that realistically describe the TDR system response. The optimization criteria are based on matching the simulated TDR waveform to those of the actual measurements. During the calibration process, the TDR system is divided into four parts: the front panel, the cable, the coaxial head, and the probe. Parameters for each part are optimized in a progressive fashion. The initial values for system parameters are estimated from the geometries and documented material properties. The steps in the calibration procedure include

1. Calibration of the front panel. The target TDR signal was acquired with the front panel terminated by a 50 Ω impedance block. The front panel is then modeled with 30 segments. Values of the impedance and the lengths for these segments are obtained from matching the predicted signal with the target signal. The initial impedance is set to 50 Ω for each section, and the initial length of each section is set to be 0.01 m.
2. Calibration of the coaxial cable. The target TDR signal was acquired with the cable connected and terminated with a 50 Ω impedance block. The length of the cable is physically measured. The impedance and the dielectric parameters of the insulating material for the cable are then found by optimization.
3. Calibration of the probe head and the measurement probe. The target TDR signal was acquired in the cylindrical mold filled with deionized water, and the length and impedance of the coaxial head and measurement probe were calibrated.

For each step, a least-squares-error function is defined as

$$\text{Error} = \sum (M_i^{\text{obs}} - M_i^{\text{calc}})^2; \quad i = N_0 \quad \text{to} \quad N_E \tag{15}$$

where M_i^{obs} and M_i^{calc}=measured and simulated signals; N_0 and N_E=points where the reflection of the section to be optimized starts.

The objective of each step of the optimization is to minimize the error function in Eq. (15). The optimizations are performed with a simplex search method (Lagarias et al. 1998), which is a subroutine in MATLAB.

Table 1 presents the optimized system parameters of the cable, the coaxial head, the air gap, and the probe. Fig. 7 shows the measured waveform for deionized water as well as the simulated waveform using the optimized parameters. The simulated waveform closely matches the measured waveform.

Surface Reflection Dielectric Constant from Simulated Surface Reflections

After the TDR system has been calibrated, the system parameters can be used in the subsequent waveform simulation to determine the dielectric permittivity of soils with high electrical conductivities using the reflection from the surface of the soils. An important issue is to determine the range of the signal to be matched, as required to calculate the error function Eq. (15). From the system

Table 1. Parameters of the Cable, Coaxial Head, Air Gap, and Probe from Calibration

Sections	Number of sections	Characteristic impedances Z_p, Ω	Lengths l, cm	Debye parameters			DC conductivities σ_{DC}, ms/m
				ε_s	ε_∞	f_r, Hz	
Cable	1	71.6	184	2.16	2.10	1.0×10^8	0
Coaxial head	2	87.2, 200	3.13, 3.69	4.13	2.98	9.6×10^8	0
Air gap	2	120.9, 280	3.51, 1.10	1	1	NA	0
Cylindrical mold probe	1	153.4	11.6	NA	NA	NA	NA

calibration process, the reflections from the coaxial head, the air gap, and the surface of materials can be identified from the impulse TDR signal.

The start of the matching range should be the first point where the first reflection from the surface occurs. However, the first reflection from the surface of the material overlaps with the reflection from the air gap for the probe heads used in this research. This makes it difficult to find the actual starting point of the first reflection on the waveform. Hence, point A in Fig. 5(a), which is more easily determined and is close to the starting point of the first reflection, is selected. The end of the matching range can theoretically be any point before the arrival of the reflection from the probe end, as long as the range is sufficiently large.

However, the probe and the coaxial head tend to filter out the high-frequency components, which reduce the upper limit of the frequency bandwidth of the reflected signal. Considering this factor, the end of the first reflection from the soil surface [point 4 in Fig. 5(b)] is used to set the end of the range in the waveform matching during the optimization process. The range of waveform matching is shown in Fig. 5(a) from point A to point B. The bulk DC electrical conductivity in Eq. (14) is determined from the long-term signal level, and therefore the surface reflection dielectric constant, K_{aSR}, is the only parameter to be inverted. The initial value of K_{aSR} can be assumed to be any value between 3 and 100.

As a validation of this approach, TDR waveforms for water with different sodium chloride concentrations were used. The electrical conductivities range from 0 mS/m for deionized water to 476 mS/m for highly salty water. The initial K_{aSR} were set to be 10. The measured waveforms and the waveforms computed with the inverted K_{aSR} are plotted in Fig. 8. Overall, the waveforms match closely. The inverted K_{aSR} values of salty water are close to the value for deionized water. For example, when the ion concentration of NaCl solution is 0.1 mol/L (σ_{DC}=1,060 mS/m at 20°C, an exceptionally high electrical conductivity), the real dielectric permittivity at 1 GHz decreases almost 1.5% in comparison to the deionized water (Santamarina et al. 2001). The highest electrical conductivity of the salty water studied in this paper is 467 mS/m. Hence, the ion concentration doesn't have a significant impact on the K_{aSR} for the material studied in this research, validating the assumptions used in this model.

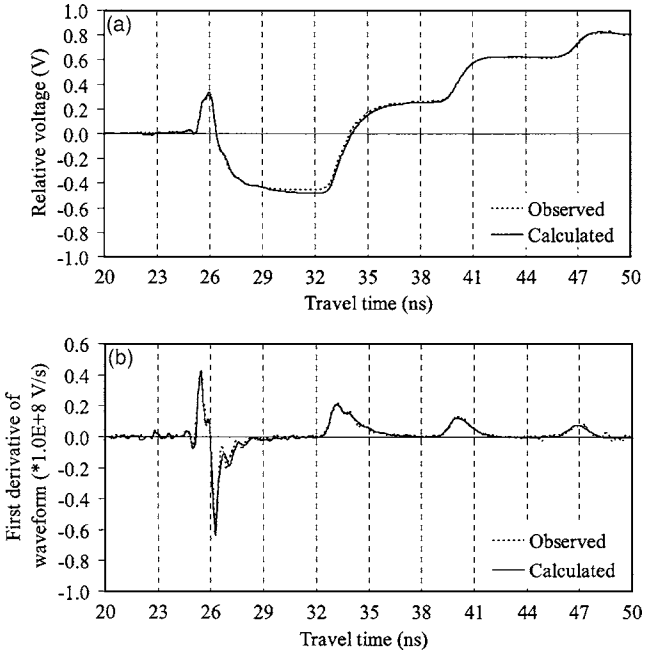

Fig. 7. Measured and predicted TDR waveforms for deionized water: (a) step response; (b) impulse response calculated from step response

Experiments and Results

Materials and Methods

Lime kiln dust (LKD) is a by-product of the lime industry. Since LKD makes stabilization of soils economical and has the added advantage of recycling a by-product, it has been extensively used for stabilizing subgrades to facilitate construction and enhance the engineering properties of soils. Within a few days after stabilization (typically less than 3 days), field tests are conducted to measure the dry density and water content of soils to assess the compaction quality.

Addition of lime to soil involves complicated chemical reactions (Diamond and Kinter 1965). Yu and Drnevich (2004b) applied the TDR technology to the measurement of the water content and density of the lime and fly ash-modified soils with satisfactory accuracy. However, the measurement of the dielectric

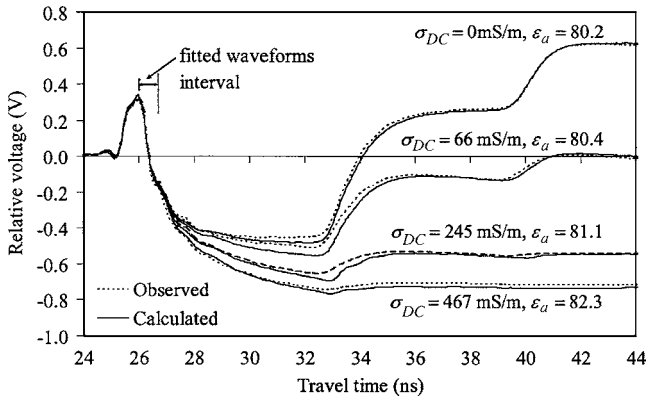

Fig. 8. Measured and predicted TDR waveforms for water with different electrical conductivities; values were inverted using an optimization approach

Table 2. Summary of the Experimental Program and Results for LKD Modified Grundite

Specimen name[a]	LKD added (%)	Water content (%)		Dry density (Mg/m^3)	K_{aSR}	w (%) from K_{asR}	K_a[b]	w(%) from K_{aSR}	σ_{DC} (mS/m)	Time[c]
		After compaction	After monitoring							
G15-13	15%	13.56%	13.40%	1.622	12.2	13.8%	16.2	17.5%	89.2	5 mins
					10.5	12.0%	14.8	16.3%	67.4	2 h
					9.5	10.9%	11.9	13.5%	40.3	74 h
G15-17	15%	17.23%	16.67%	1.735	18.8	17.7%	NA	NA	172.7%	5 mins
					14.7	14.4%	NA	NA	142.6%	26 h
					15.9	15.4%	19	17.9%	71.2	111 h
G15-21	15%	20.88%	20.87%	1.787	26	21.8%	NA	NA	242.4%	5 mins
					23.2	20.0%	NA	NA	164.3%	6 hr
					22.5	19.5%	21	18.5%	115.9	63 h
G11-13	11%	12.62%	12.71%	1.658	13.1	14.1%	13.8	14.8%	67.3	5 mins
					13.1	14.1%	12.2	13.3%	56.6	1 hr
					13.1	14.1%	10.7	11.7%	34	69 h
G11-17	11%	17.13%	17.21%	1.737	21.98	20.0%	NA	NA	139.3	5 mins
					18.8	17.7%	NA	NA	116.5	1 hr
					16.5	15.9%	19	17.9	73.6	74 h
G11-21	11%	20.21%	20.41%	1.765	24.8	21.4%	NA	NA	174.8	5 mins
					20.5	18.5%	21.1	18.9%	142.3	1 h
					18.5	17.0%	19.3	17.6%	82.4	71 h

[a]The first number in the specimen name indicates the LKD percentage by dry weight of soil; the second number indicates the target water content of the mixture just after compaction.

[b]K_a as measured by travel time analysis.

[c]Time indicates when the measurement was taken after compaction.

constant is challenging for the cases of high chemical dosage and high water content of the parent soil, because in those situations the electrical conductivity is high enough to attenuate the reflected signal. Fortunately, the electrical conductivity continues to decrease with time due to the chemical reactions occurring in the mixture.

TDR monitoring was implemented to find the change in the electrical conductivity and dielectric constant with time in this study. Grundite, an illitic clay, was used in the experiments. The grundite was mixed using tap water to achieve a target water content. The sample was then sealed in plastic bags and placed for 24 h in a room with a constant temperature of around 22°C. On the following day, a specific amount of LKD, based on the weight of the soil solids, was added and mixed using a mechanical mixer for 5 min. The mixture of grundite and LKD was compacted in the cylindrical mold in accordance with ASTM D 698a (ASTM 2000). After compaction, the surface of the mixture in the cylinder was sealed with wax to prevent moisture evaporation.

Measurements were taken automatically every hour using the in-house TDR apparatus (Daita et al.. 2005). The water contents of the mixture just after compaction and monitoring were measured by the oven-dry method for ASTM D 2216 (ASTM 2005a). A summary of the experimental program is presented in Table 2. Six specimens, three with 11% LKD and three with 15% LKD each, were monitored with target water contents of 13, 17, and 21%. The monitoring of the specimens was conducted up to about 3 days because the short-term behavior of the LKD-modified soils was of interest and field tests for quality control are usually done within 3 days. The TDR waveforms of the specimens measured at three different curing times were analyzed using the method developed in this paper.

Results and Discussion

The waveforms of specimen G15-21 taken at three different times are plotted in Fig. 9. The addition of LKD to the soil increases the electrical conductivities of the specimens due to the increased amount of free ions, and the increase in temperature is caused by hydration reactions. The high electrical conductivities make the measurements of the apparent dielectric constants difficult within the first day after compaction as the second reflection is indiscernible. After some time, the electrical conductivity decreases and the second reflections in the TDR waveforms become apparent. The curing processes in the LKD-modified soils don't appear to

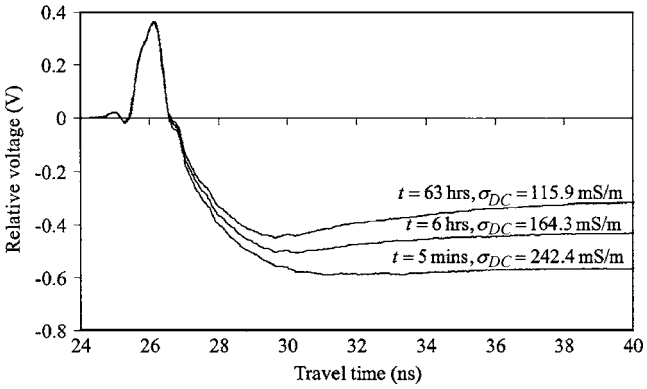

Fig. 9. Measured waveforms in 15% LKD-modified grundite with target water content of 21% at three different times

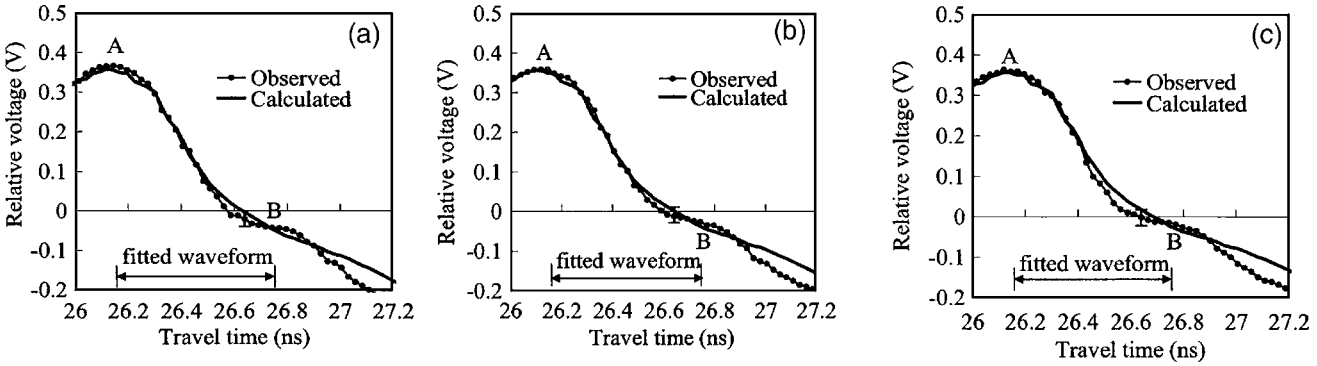

Fig. 10. Measured and calculated waveforms for 15% LKD-modified grundite with target water content of 21% at (a) t=5 min (σ_{DC}=242 mS/m); (b) t=6 h (σ_{DC}=164 mS/m); (c) t=63 h (σ_{DC}=116 mS/m) after compaction. Vertical bars show two standard deviations expected in TDR waveforms within fitted range, based on 30 measurements made on deionized water.

change the water content from the measured water contents just after compaction and after completion of the monitoring program.

The model matching method based on the surface reflection presented earlier in this paper was used to invert for the dielectric constants. Fig. 10 presents the inverted waveforms and the measured waveforms of specimen G15-21 with different times (electrical conductivities) after compaction. To evaluate the quality of the optimization, 30 measurements were made on a specimen consisting of only deionized water. The standard deviation of measured TDR waveforms over the same range in Fig. 10 was around 0.021 V. The vertical bars in Fig. 10 are two standard deviations of the variations in the results of inversion analysis on the experimental signals for deionized water.

An observation can be made that the waveforms have a close match within the first reflection from the soil surface (from points A to B in Fig. 10), but the errors continue to increase toward point B due to multiple reflections from within the probe head. The amplitudes of the predicted waveforms are larger than those of the measured values for times greater than point B, which is probably due to the use of the simplified model for the inversion that does not account for the imaginary part of dielectric permittivity.

Table 2 summarizes the measured (K_a) and inverted (K_{aSR}) dielectric constants for all specimens at different curing times. The dielectric constants obtained from both travel time and inversion analyses indicate a slight decrease of dielectric constant with time after compaction. This may be due to immobilization of some of the pore water from the hydration taking place. In Table 2, the inverted dielectric constants are for the most part lower than those obtained from the travel time analysis. This is consistent with Topp et al. (2000) and Jones and Or (2004), who found that the apparent dielectric constant estimated from travel time analysis increases with increasing electrical conductivity.

The high electrical conductivity flattens out the reflection from the probe end, which results in a higher estimation of the apparent dielectric constant (Fig. 8). As given by Eq. (14), the effect of DC electrical conductivity is included in the optimization, but the influence of the DC electrical conductivity on the dielectric constant determination is excluded with the proposed inversion procedure. Note that Eq. (14) does not consider the effects of the imaginary part of the dielectric permittivity, which means the loss of energy is underestimated. This can be found by the separation of the inverted and measured waveforms beyond the fitted time interval in Fig. 10.

Another reason for the differences between dielectric permittivities from travel time and from inversion could be due to the permittivity near the soil surface being somewhat different from the overall permittivity of the specimen due to surface drying or accumulation of moisture. Additional work is needed to document the impact of these conditions on calculated apparent dielectric permittivity from surface reflections.

Siddiqui and Drnevich (1995) developed a calibration equation [Eq. (16)] that relates the apparent dielectric constant of soils to the gravimetric water content

$$\sqrt{K_a}\frac{\rho_w}{\rho_d} = a + bw \tag{16}$$

where ρ_w=density of water; ρ_d=dry density of the soil; and a and b are soil-dependent calibration constants.

Tests on five soil mixtures provided average values of a=0.945 and b=8.76 (Drnevich et al. 2005). Using these two parameters and the measured dry densities as given in Table 2, the water contents of the different samples can be estimated for both K_a and K_{aSR}, where K_{aSR} is substituted for K_a in Eq. (16). The results are compared in Fig. 11 against the water contents mea-

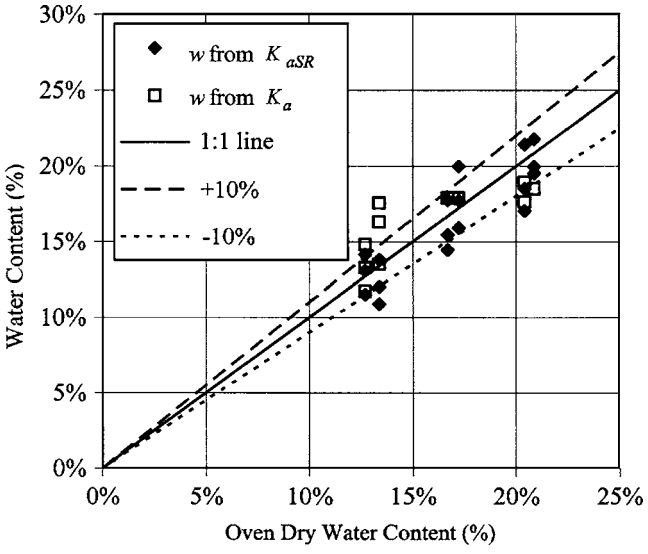

Fig. 11. Water content from apparent dielectric constant (K_a) by travel time analysis and from dielectric constant (K_{aSR}) from model-based inversion procedure compared to oven dry water contents for grundite with differing amounts of LKD

sured by oven drying. Examination of Table 2 and Fig. 11 indicates that the water contents from K_a are larger than corresponding ones calculated with K_{aSR}. The reason for this is that the apparent dielectric constant by travel time analysis includes the contribution of electrical conductivity, while results for the inversion using Eq. (14) provide K_{aSR}, which is independent of electrical conductivity.

For soils with low values of electrical conductivity, results will be almost the same. For this reason, use of K_{aSR} should be more accurate for water content determination for highly conductive soils. In addition, the waveform matching methods still work satisfactorily for situations where the conventional travel time analysis fails due to weak or nonexistent second reflections. Note in Fig. 11 and Table 2 that water contents calculated by use of K_{aSR} are quite reasonable for situations where it was not possible to measure K_a. The developed new method appears to have an advantage over the conventional travel time analysis in that it can be applied to soils with high electrical conductivities where second reflections are weak or absent altogether.

Summary of Application Procedures

Measurements of dielectric permittivity and electrical conductivity using TDR are reliable and fast. This paper presents an approach for estimating the apparent dielectric constant from the reflection at the surface of soils by using a model-based inversion method. This approach can be applied to contaminated soils and chemically modified soils that have high electrical conductivities. The dielectric properties of the contaminated soils may be used to detect the migration of the contaminant components in the soils (Francisca and Rinaldi 2003). TDR is also feasible for measuring the water content and the dry density of the LKD modified soils. Changes of dielectric properties induced by chemical reactions coincide with the strength development of the modified soils. Test results indicate that electrical conductivity also can be correlated to penetration resistance of modified soil, which is an indicator of the shear strength (Daita et al. 2005). The use of TDR is expected to be able to provide a better understanding of the rate and extent of chemical reactions between chemical modifiers such as LKD and soil and to be useful for compaction quality control.

To apply the approach proposed herein, the progressive calibration of transmission components is implemented first. For the equipment described in ASTM D 6780 (ASTM 2005b), the calibration includes the front panel, cable, coaxial head, and probe. The reflections from the different sections are identified using the impulse response; then the waveform for high-conductive soil is measured in accordance with ASTM D 6780 (ASTM 2005b). The bulk DC electrical conductivity is calculated using the approach of Giese and Tiemann (1975). Eq. (14) is utilized to describe the dielectric permittivity of soil for the inversion process. The error function [Eq. (15)] is used as the criterion for the optimization, in which the range for matching data points should be constrained only to those for the first reflection from the soil surface. The prior value for estimating the apparent dielectric constant in Eq. (14) is set to any number between 3 and 100, and the final value is found by optimization.

Conclusions

A progressive calibration of transmission line components of a TDR system is presented and is based on the theory of nonuniform transmission lines. The reflection of the TDR signal from the soil surface is used to invert for the apparent (high-frequency) dielectric constant. The approach was validated with the experimental data on saline water and LKD-modified soils. Major conclusions from this investigation include

- The impedance mismatches in the TDR system enhance the overlap of reflections from different parts of the TDR probe. For travel time analysis, the peak point on the waveform of the reflection signal is influenced by the dielectric constant of the material being tested with the probe and the length of the air gap. Measurements on materials with small dielectric constants will cause a slightly delayed peak point on the step response and results in an underestimate of the dielectric constant. Alternative approaches are proposed to find the first reflection from the impulse response.
- With nonuniform transmission line theory, the system parameters of the TDR can be calibrated progressively from the front panel to the probe. The dielectric constant can then be obtained from the surface reflection with a frequency-independent dielectric permittivity model. The inverted and measured waveforms have a good match within the first reflection from the specimen surface, but the differences continue to increase when the multiple reflections within the TDR probe head appear.
- For the LKD-modified soils studied in this paper, the inverted dielectric constants are lower than those obtained from travel time analysis. The variations of water content estimated with the dielectric constants obtained by the two approaches are within the acceptable limits for the purpose of engineering applications.
- The electrical conductivities of LKD-treated grundite measured with TDR decrease dramatically with time after compaction, while the dielectric constants only change slightly. The inverted dielectric constants from the TDR waveforms measured just after compaction (where travel time analysis fails to work) are consistent with the trend of the dielectric constants measured with travel time analysis after the specimens were cured for a period of time.
- TDR can be used to estimate the dry density and water content of soils with high electrical conductivities. The decrease of electrical conductivity is correlated to the increase of the strength of the LKD-modified soil. Hence, the use of TDR could provide a better understanding of the rate and extent of chemical reactions between chemical modifiers [e.g., lime and lime kiln dust (LKD)] and soils. TDR can be a useful tool for compaction quality control of stabilized soils.

Acknowledgments

The first writer gratefully acknowledges research funding from the Board of Pao's Scholarship for Chinese Students to Study Abroad, and all the writers appreciate the support of the Chinese Natural Science Foundation, Project No. 50308026, and the U.S. National Science Foundation, Project No. CMS-0244704. Any opinions, findings, and conclusions or recommendations expressed in this material are those of the writers and do not necessarily reflect the views of the Chinese Natural Science Foundation or the U.S. National Science Foundation.

Notation

The following symbols are used in this paper:

a, b = soil-dependent calibration constants for water content estimation;
C = constant related to probe configuration for estimating electrical conductivity;
c = velocity of light in vacuum (2.998×10^8 m/s);
$Error$ = least-square-error function in the optimization;
f = frequency;
f_r = relaxation frequency of the material;
K_a = apparent dielectric constant measured by travel time analysis;
K_{aSR} = apparent dielectric constant measured by surface reflection analysis;
$K^*(\omega)$ = relative complex dielectric permittivity;
$K'(\omega)$ = real part of the relative dielectric permittivity;
$K''(\omega)$ = imaginary part of the relative dielectric permittivity;
L_p = length of the probe;
M_i^{obs} = ith observed data of TDR waveform;
M_i^{calc} = ith calculated data of TDR waveform;
N_E = point where reflection of segment to be optimize ends;
N_0 = point where reflection of segment to be optimized starts;
V^+, V^- = two unknown voltage constants;
V_s = TDR source voltage;
$V(0)$ = TDR sampling voltage;
w = gravimetric water content;
Z_c = characteristic impedance of line;
Z_L = TDR load impedance;
$Z_{in}(z_i)$ = input impedance that is the equivalent impedance when looking into the circuit at position z_i;
Z_p = reference characteristic impedance of transmission line insulated with air;
Z_s = TDR source impedance;
z = position along transmission line;
γ = wave propagation constant;
ε_s = static dielectric permittivity;
$\varepsilon^*(\omega)$ = complex dielectric permittivity;
ε_0 = dielectric permittivity of free space (8.854×10^{-12} F m^{-1});
ε_∞ = dielectric permittivity at an infinite frequency;
ρ_d = dry density of soil;
ρ_w = density of water;
σ_{DC} = bulk DC electrical conductivity; and
ω = angular frequency ($\omega = 2\pi f$).

References

ASTM. (2000). "Standard test methods for laboratory compaction characteristics of soil using standard effort." *D 698-00a*, West Conshohocken, Pa.

ASTM. (2005a). "Standard test method for laboratory determination of water (moisture) content of soil and rock by mass." *D 2216*, West Conshohocken, Pa.

ASTM. (2005b). "Standard test method for water content and density of soil in place by time domain reflectometry (TDR)." *D 6780-05*, West Conshohocken, Pa.

Benson, C. H., and Bosscher, P. J. (1999). "Time-domain reflectometry (TDR) in geotechnics: A review." *ASTM special technical publication*, 1350, 113–136.

Chen, R. P., Daita, R. K., Drnevich, V. P., and Kim, D. H. (2006). "Laboratory TDR monitoring of physico-chemical process in lime kiln dust stabilized clayey soil." *Chinese J. Geotech. Eng.*, 28(2), 249–255.

Clarkson, T. S., Glasser, L., Tuxworth, R. W., and Williams, G. (1977). "An appreciation of experimental factors in time-domain spectroscopy." *Adv. Mol. Relax. Interact. Processes*, 10(3), 173–202.

Daita, R. K., Drnevich, V. P., and Kim, D. H. (2005). "Family of compaction curves for chemically modified soils." *FHWA/IN/JTRP-2005/7*, Purdue Univ., West Lafayette, Ind.

Debye, P. (1929). *Polar molecules*, Chemical Catalog Company, New York.

Diamond, S., and Kinter, E. B. (1965). "Mechanisms of soil-lime stabilization: An interpretive review." *Highway Research Record No. 92*, Highway Research Board, National Research Council, Washington, D.C., 83–103.

Drnevich, V. P., Ashmawy, A. K., Yu, X., and Sallam, A. M. (2005). "Time domain reflectometry for water content and density of soils: Study of soil-dependent calibration constants." *Can. Geotech. J.*, 42, 1053–1065.

Drnevich, V. P., Lin, C. P., Yi, Q., Yu, X., and Lovell, J. (2001). "Real time determination of soil type, water content and density using electromagnetics." *Rep. No. FHWA/IN/JTRP-2000-20*, Joint Transportation Research Program, Indiana Dept. of Transportation-Purdue Univ. ⟨http://rebar.ecn.purdue.edu/jtrp/final-report/spr-2201-final-form1700.pdf⟩.

Fellner-Feldegg, H. (1969). "The measurement of dielectrics in the time domain." *J. Phys. Chem.*, 73(3), 616–623.

Feng, W., Lin, C. P., Deschamps, R. J., and Drnevich, V. P. (1999). "Theoretical model of multisection time domain reflectometry measurement system." *Water Resour. Res.*, 35(8), 2321–2331.

Francisca, F. M., and Rinaldi, V. A. (2003). "Complex dielectric permittivity of soil-organic mixtures (20 MHz–1.3 GHz)." *J. Environ. Eng.*, 129(4), 347–357.

Giese, K., and Tiemann, R. (1975). "Determination of the complex permittivity from thin sample time domain reflectometry improved analysis of the step response waveform." *Adv. Mol. Relax. Processes*, 7(1), 45–59.

Heimovaara, T. J. (1994). "Frequency domain analysis of time domain reflectometry waveforms. I: Measurement of the complex dielectric permittivity of soils." *Water Resour. Res.*, 30(2), 189–199.

Heimovaara, T. J., Bouten, W., and Verstraten, J. M. (1994). "Frequency domain analysis of time domain reflectometry waveforms. II: A four-component complex dielectric mixing model for soils." *Water Resour. Res.*, 30(2), 200–210.

Hilhorst, M. A., and Dirkson, C. (1994). "Dielectric water content sensors: Time domain versus frequency domain." *Symp. and Workshop on Time Domain Reflectometry in Environmental, Infrastructure and Mining Applications*, SP 19–94, 23–33.

Jones, S. B., and Or, D. (2004). "Frequency domain analysis for extending time domain reflectometry water content measurement in highly saline soils." *Soil Sci. Soc. Am. J.*, 68(5), 1568–1577.

Krauss, J. D. (1984). *Electromagnetics*, McGraw-Hill, New York.

Lagarias, J. C., Reeds, J. A., Wright, M. H., and Wright, P. E. (1998). "Convergence properties of the Nelder-Mead simplex method in low dimensions." *SIAM J. Optim.*, 9(1), 112–147.

Lin, C. P. (2003). "Analysis of nonuniform and dispersive time domain reflectometry measurement systems with application to the dielectric spectroscopy of soils." *Water Resour. Res.*, 39(1), SBH61–SBH611.

Noborio, K. (2001). "Measurement of soil water content and electrical conductivity by time domain reflectometry: A review." *Comput. Electron. Agric.*, 31(3), 213–237.

Ramo, S., Whinnery, J. R., and van Duzer, T. (1994). *Fields and waves in communication electronics*, 3rd Ed., Wiley, New York.

Santamarina, J. C., Klein, K. A., and Fam, M. A. (2001). *Soils and waves*, Wiley, New York.

Siddiqui, S. I., and Drnevich, V. P. (1995). "Use of time domain reflec-

tometry for the determination of water content and density of soil." *FHWA/IN/JHRP-95/9*, Purdue Univ., West Lafayette, Ind.

Svitzky, A., and Golay, M. J. E. (1964). "Smoothing and differentiation of data by simplified least squares procedures." *Anal. Chem.*, 36(8), 1627–1639.

Timlin, D. J., and Pachepsky, Y. A. (1996). "Comparison of three methods to obtain the apparent dielectric constant from time domain reflectometry wave traces." *Soil Sci. Soc. Am. J.*, 60, 970–977.

Topp, G. C., Davis, J. L., and Annan, A. P. (1980). "Electromagnetic determination of soil water content: Measurements in coaxial transmission lines." *Water Resour. Res.*, 16, 574–582.

Topp, G. C., Yanuka, M., Zebchuk, W. D., and Zegelin, S. (1988). "Determination of electrical conductivity using time-domain reflectometry: Soil and water experiments in coaxial lines." *Water Resour. Res.*, 24, 945–952.

Topp, G. C., Zegelin, S., and White, I. (2000). "Impacts of the real and imaginary components of relative permittivity on time domain reflectometry measurements in soils." *Soil Sci. Soc. Am. J.*, 64(4), 1244–1252.

Van Gemert, M. J. C., and De Graan, J. G. (1972). "Calculations on the time-domain reflection behaviour of a transmission line partly filled with a polar dielectric." *Appl. Sci. Res.*, 26(1–2), 1–17.

von Hippel, A. R., ed. (1954). *Dielectric materials and applications*, MIT Press, Cambridge, Mass.

Yanuka, M., Topp, G. C., Zegelin, S., and Zebchuk, W. D. (1988). "Multiple reflection and attenuation of time domain reflectometry pulses: Theoretical considerations for applications to soil and water." *Water Resour. Res.*, 24, 939–944.

Yu, X., and Drnevich, V. P. (2004a). "Soil water content and dry density by time domain reflectometry." *J. Geotech. Geoenviron. Eng.*, 130(9), 922–934.

Yu, X., and Drnevich, V. P. (2004b). "Time domain reflectometry for compaction control of stabilized soils." *Transportation Research Record. 1868*, Transportation Research Board, Washington, D.C., 14–22.